frontiers in Astronomy and Space Sciences

BRIEF RESEARCH REPORT
published: 29 March 2021
doi: 10.3389/fspas.2021.625230

Robo-AO and SOAR High-Resolution Surveys of Exoplanet Hosting Stars

Carl Ziegler[1], Nicholas Law[2], Christoph Baranec[3], Reed Riddle[4] and Andrei Tokovinin[5]*

[1]Department of Physics, Engineering and Astronomy, Stephen F. Austin State University, Nacogdoches, TX, United States, [2]Department of Physics and Astronomy, University of North Carolina at Chapel Hill, Chapel Hill, NC, United States, [3]Institute for Astronomy, University of Hawaiʻi at Mānoa, Hilo, HI, United States, [4]Division of Physics, Mathematics, and Astronomy, California Institute of Technology, Pasadena, CA, United States, [5]Cerro Tololo Inter-American Observatory, La Serena, Chile

In the past decade, space-based transit surveys have delivered thousands of potential planet-hosting systems. Each of these needs to be vetted and characterized using follow-up high-resolution imaging. We perform comprehensive imaging surveys of the candidate exoplanets detected by the Kepler and TESS missions using the fully autonomous Robo-AO system and the largely autonomous SOAR speckle imaging system. The surveys yielded hundreds of previously unknown close binary systems hosting exoplanets and resulted in verification of hundreds of exoplanet systems. Evidence of the interaction between binary stars and planetary systems was also detected, including a deep deficit of planets in close binary systems.

Keywords: exoplanets, adaptive optics, speckle interferometry, binary stars, high-resolution imaging

OPEN ACCESS

Edited by:
Steve B. Howell, National Aeronautics and Space Administration (NASA), United States

Reviewed by:
Luca Fossati, Austrian Academy of Sciences, Austria
John Livingston, The University of Tokyo, Japan

****Correspondence:***
Carl Ziegler
carl.ziegler@sfasu.edu

Specialty section:
This article was submitted to Exoplanets, a section of the journal Frontiers in Astronomy and Space Sciences

Received: *02 November 2020*
Accepted: *08 January 2021*
Published: *29 March 2021*

Citation:
Ziegler C, Law N, Baranec C, Riddle R and Tokovinin A (2021) Robo-AO and SOAR High-Resolution Surveys of Exoplanet Hosting Stars. Front. Astron. Space Sci. 8:625230. doi: 10.3389/fspas.2021.625230

1 INTRODUCTION

Over the past decade, the Kepler telescope (Borucki et al., 2010) and its follow-up mission, the Transiting Exoplanet Survey Satellite (TESS, Ricker et al., 2014), have detected the majority of known exoplanets. Each satellite consists of high-precision photometers, able to measure the brightness of thousands of stars simultaneously. A planet passing in front of one of these stars as seen from Earth, a transit, will result in a slight dip in brightness (the size of the dip being related to relative sizes of the planet and star). Periodic dimming of a star is therefore potential evidence of an orbiting exoplanet.

The addition of a second star in the system, so that the light from both is blended together, results in a shallower brightness dip during transit. The size of the planet, which is estimated based on the depth of the brightness dip, is biased small when the light from a second object is included. The nearby star may actually be an eclipsing binary system. When blended with the brighter target star, the large dips from the eclipsing stars may result in a planet-like signal. Both the Kepler and TESS missions were blind to wide binary stars, which were not removed from either Kepler (Brown et al., 2011) or TESS (Stassun et al., 2019) input catalogs. The majority of close binary stars (those within an arcsecond of separation) are not known in advance due to the typically low-resolution of seeing-limited observations and the resolution limit of Gaia DR2 (Ziegler et al., 2018b).

Resolving close binary systems requires high-resolution imaging from the ground. Conventional systems, such as laser GuideStar adaptive optics (LGS-AO) instruments, require long overheads before observations can begin, typically on the order of 15–20 min [e.g., Keck-AO (Wizinowich et al., 2006)], and are generally only available on large telescopes (apertures greater than 8 m). With thousands of targets requiring such observations, approximately a hundred dedicated nights would be required to complete a comprehensive survey. Practically, this is outside the allocated time that will be provided for this purpose. In the first few years of the Kepler mission, the follow-up campaign proceeded with a patchwork of smaller surveys performed on different telescopes observing in both

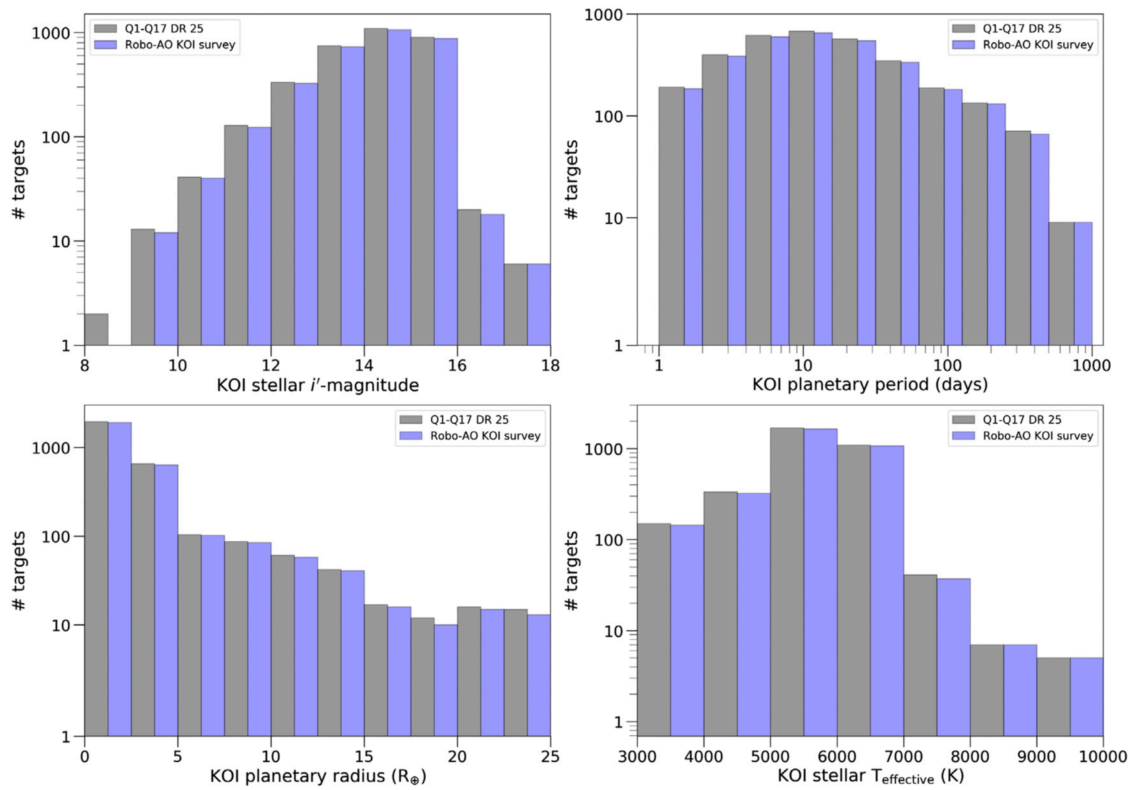

FIGURE 1 | The properties of KOIs observed in the Robo-AO survey are compared to the full set of KOIs from Q1–Q17 (Borucki et al., 2010; Borucki et al., 2011a; Borucki et al., 2011b; Batalha et al., 2013; Burke et al., 2014; Rowe et al., 2014; Coughlin et al., 2016; Mathur et al., 2017).

visible and infrared bands (Howell et al., 2011; Adams et al., 2012; Adams et al., 2013; Horch et al., 2012; Lillo-Box et al., 2012; Dressing et al., 2014; Horch et al., 2014; Lillo-Box et al., 2014; Marcy et al., 2014). These disparate sources of data limited the broad statistical studies that could be performed to understand how planets form and evolve in tight binary systems.

A high-resolution instrument which also has high observing efficiency is therefore required to perform such a large survey. Through full automation, Robo-AO achieves observing time efficiencies that are an order-of-magnitude greater than those of conventional high-resolution instruments. Between 2012 and 2016, Robo-AO was used by our team to observe every Kepler Object of Interest (KOI) system (Law et al., 2014; Baranec et al., 2016; Ziegler et al., 2017; Ziegler et al., 2018a; Ziegler et al., 2018c). These observations were typically sensitive to nearby stars as close as the diffraction limit of the telescope (approximately 0.15″) and to stars up to six magnitudes fainter than the target star. Within this survey, nearly 95% of Kepler planetary candidates host stars (3,857 KOIs in total) were observed, and 620 stars with separations less than a few arcseconds were detected.

Beginning in late 2018 and continuing to present, the Southern Astrophysical Research telescope (SOAR) has performed speckle observations of TESS planet candidates. Speckle imaging on SOAR typically reaches the diffraction limit on bright targets ($V < \sim 12$), including most TESS targets (TESS Objects of Interest, or TOIs), and the observation sequence is optimized to be capable of up to 300 observations a night (Tokovinin, 2018). The first results from this survey, covering 542 TESS targets with 117 detected companions, was recently published in Ziegler et al., (2020). Additional 357 TESS targets observed by SOAR will be presented in an upcoming work.

This article provides a summary of the surveys and their results. We describe in detail the observations from each instrument in **Section 2** and summarize the results of the surveys in **Section 3**. We conclude in **Section 4**.

2 OBSERVATIONS

2.1 Robo-AO

The objective of the Robo-AO Kepler survey was to take image in high-resolution of every candidate planet host star detected by the Kepler telescope. We therefore targeted every KOI from the available data releases (culminating with the Kepler DR25 catalog based on Q1-Q17 data) (Borucki et al., 2010; Borucki et al., 2011a; Borucki et al., 2011b; Batalha et al., 2013; Burke et al., 2014; Rowe et al., 2014; Coughlin et al., 2016; Mathur et al., 2017). We removed KOIs that were flagged as false positives using Kepler data at the time of the observation runs.

The properties of targeted KOIs in the Robo-AO survey are presented in **Figure 1**. The distributions in magnitude, planetary radius, planetary orbital period, and stellar temperature of the

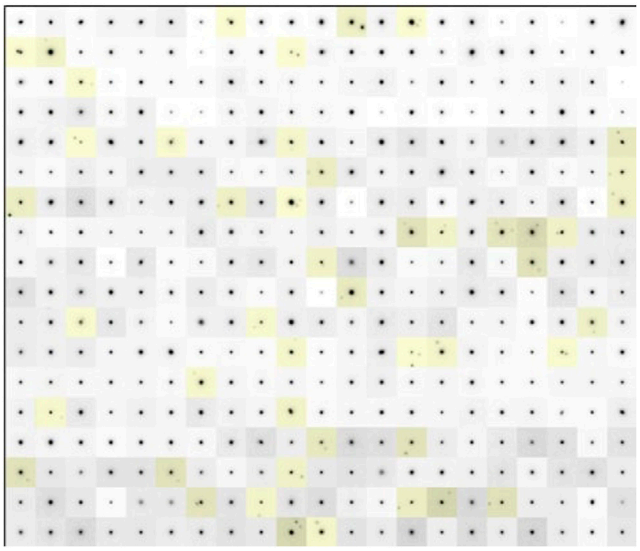

FIGURE 2 | Robo-AO centered cutout images of Kepler planetary candidate host stars. Systems with discovered nearby stars are highlighted. Shown are ~10% of the targets from the Robo-AO survey of KOIs, the largest adaptive optics survey of exoplanet hosts yet performed. Results from this survey have been used to validate over a thousand planets.

observed stars are similar to the full set of KOIs from Q1 to Q17 that have CANDIDATE dispositions based on only Kepler data. This is a result of the comprehensive nature of this survey. An example of the Robo-AO images within this survey is presented in **Figure 2**.

The Robo-AO instrument was mounted on telescopes at Palomar and Kitt Peak during the course of this survey (Baranec et al., 2014b; Baranec et al., 2017; Jensen-Clem et al., 2018). To correct high-order wavefront aberrations introduced by atmospheric turbulence, the adaptive optics system of Robo-AO runs at a loop rate of 1.2 kHz. The delivered performance of the system (median Strehl ratios of 9% and 4% in the i'-band at Palomar and Kitt Peak) allowed identification of companion stars down to the diffraction limit of the telescope. A long-pass filter that cuts on at 600 nm (LP600) was used for observations of the KOI targets. This filter is a good approximation of the Kepler bandpass at redder wavelengths, while also reducing the blue wavelengths that reduce the performance of the adaptive optics correction. A comparison of the LP600 passband to the Kepler passband is presented in **Figure 1** of Law et al., (2014). The majority of the survey (3,313 KOIs) was performed with Robo-AO mounted on the Palomar 1.5 m telescope between 2012, July 16 and 2015, June 12 (UT). An additional 532 KOIs were observed with Robo-AO mounted on the Kitt Peak 2.1 m telescope between 2016, June 8 and 2016, July 15 (UT).

The Robo-AO system achieves a typical FWHM resolution of 0.15″ (at the diffraction limit). An electron-multiplying CCD (EMCCD) is used to record the images. This camera allows short frame rates, useful for software corrections for tip and tilt using a faint ($m_V < 16$) natural guide star in the field of view. In **Table 1** we summarize the specifications for the Robo-AO KOI survey.

TABLE 1 | The specifications of the Robo-AO KOI survey.

KOI targets	3,857
FWHM resolution	~0.15” (@600–750 nm)
Observation wavelengths	600–950 nm
Detector format	$1{,}024^2$ pixels
Pixel scale	43 mas/pix (palomar) 35 mas/px (kitt peak)
Exposure time	90 s
Targets observed/hour	20
Observation dates At palomar 1.5 m	2012 July 16 – 2015 June 12
Observation dates At Kitt peak 2.1 m	2016 June 8 – 2016 July 15

A currently in-development Robo-AO 2 system (Baranec et al., 2014a) mounted on the UH-88 in telescope on Maunakea will be used in the future to take image in high-resolution of Northern TESS planet candidate hosts.

2.2 SOAR Speckle Imaging

We are observing TESS planet candidate hosts with the high-resolution camera (HRCam) imager on the 4.1 m SOAR telescope. TESS targets have been observed during 13 separate runs in 2018–2020. Over the course of these observations, 95% (707) of the 742 bright ($T < 13$) candidate planet host stars from the two-year primary TESS mission that are observable from the South ($\mathrm{dec} < +20°$) have been observed in high-resolution in the SOAR TESS survey. Observations of planet candidates from the extended TESS mission are ongoing. The properties of the targeted stars are plotted in **Figure 3** and the survey specifications are listed in **Table 2**.

The observation procedure and data reduction are described in detail in Tokovinin (2018) and in Ziegler et al. (2020). In summary, an 11 s burst of 400 images is taken with an Andor iXon-888 camera. Each image consists of 200 × 200 binned pixels that are centered on the target star. The images subtend an angular region on the sky that is 6.3″ on a side, giving a plate scale of 0.01575″/pixel. A custom IDL script reduces the resulting datacube. A power spectrum is computed, and, if the target star is a binary, characteristic fringes are apparent. Modeling the power spectrum provides the separation, magnitude difference, and position angle of the companion. The Fourier transform of the power spectrum is the speckle autocorrelation function (ACF). Secondary stars will appear as mirrored peaks in the ACF, appearing at the separation and position angle of the companion. The frames in the datacube are shift-and-added, centering each on the brightest pixel, to determine the true position of the companion and remove the 180-degree ambiguity. Examples of typical speckle data are available in **Figure 4** in Tokovinin (2018). The observations in the SOAR TESS survey were taken in *I*-band. This bandpass (λ_{cen} = 824 nm, $\Delta\lambda$ = 170 nm) is similar to the bandpass used by TESS.

3 IMPACT OF BINARY STARS ON PLANETARY SYSTEMS

3.1 Binary Fractions

Within the Robo-AO Kepler survey, we found 610 stars within 4″ of 559 planetary candidate hosts (out of an observed total of 3,857

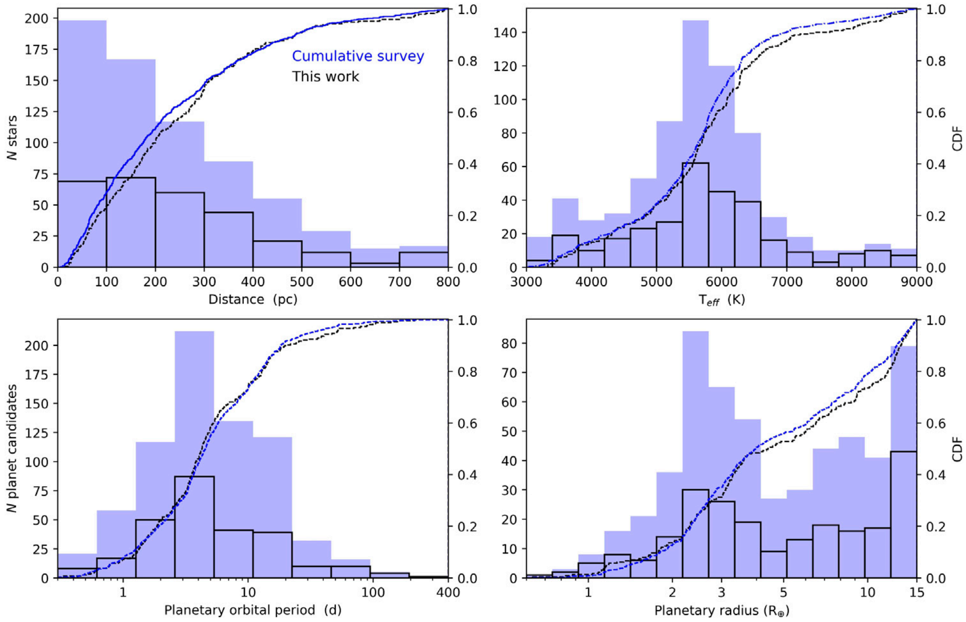

FIGURE 3 | The properties of the 653 TESS planet candidate hosts observed in the SOAR TESS survey from Ziegler et al., (2020) and in preparation (this work). A cumulative density function for each property is overplotted in black. Targets identified as known or likely false positives, 196 in total, have been removed.

TABLE 2 | The specifications of the SOAR speckle TESS survey.

TOI targets	875
FWHM resolution	~0.06″ (@700–900 nm)
Observation wavelengths	λ_c = 824 nm, $\Delta\lambda$ = 170 nm
Detector format	200^2 pixels
Pixel scale	15.7 mas/pix
Exposure time	11 s
Targets observed/hour	~30
Observation dates	2018 Oct 21—on-going

KOIs). This implies a nearby star fraction rate with the detection sensitivity of Robo-AO (separations between ~0.15″ and 4.0″ and typically $\Delta m \leq 6$) of 14.5 ± 0.6%. A triple star fraction (two additional stars within 4.0” of the target) of 1.2 ± 0.2% and a quadruple star fraction of $0.08^{+0.06}_{-0.03}\%$ were also detected.

Simulations using simulated galactic star fields and observational evidence suggest that most nearby stars at separations $< 1''$ are likely bound (Horch et al., 2014; Ziegler et al., 2018c). We find that 5.3 ± 0.3% of KOIs have another star within 1.5″ and 10.7 ± 0.5% within 3″.

The SOAR TESS survey finds companion rates to transiting exoplanet candidate hosts within 1.5″ and 3″ of 16.2 ± 1.7% and 23.2 ± 2.0% within 1.5″ and 3″, respectively.

The TESS nearby star rates are significantly higher than the Kepler rates. If we assume a physical separation distribution for binaries around exoplanet hosts as we find for field stars (Raghavan et al., 2010) which peaks at 50 AU, many more real binaries would be resolvable around TESS planet hosts (average distance of ~200 pc) compared to Kepler planet hosts (average distance of ~500 pc). The TESS system is also generally brighter (by ~3 mags on average), making fainter companions more readily detectable.

3.2 Radius Corrections

The additional flux from a stellar companion will reduce the transit depth in a photometric light curves. This dilution will result in an underestimated planetary radius. In general, it is not known which of the two stars hosts the planet in an S-type configuration (i.e., a planet in a binary system that orbits only one of the stars) (Horch et al., 2014). Gaidos et al., (2016) provide some evidence, however, that typically the primary (brightest) star is more likely to be the planet host. We therefore estimated correction factors for radius estimates for either host scenario. The detailed description of how the radii of planet candidates are corrected for the presence of a previously unknown stellar companion is provided in Ziegler et al., (2018c).

We find, for the Kepler planets, that, if we assume that all the planets orbit around the primary stars, the planetary radii increase by a factor of 1.08 on average. This factor is relatively small, as generally the companions are much fainter than the primary stars and thus the dilution of the transit is small. We found a similar correction factor for TESS planets of 1.11. Instead, if we assume all planets orbit around the secondary stars (and assuming these are not line-of-sight asterisms, but gravitationally bound to the primary), the radii of the TESS planets will increase, on average, by a factor of 2.55, slightly less than 3.29 found for Kepler planets. If we instead assume that the planet candidates are equally likely to be hosted by the primary or secondary star, we find average radius correction factors for Kepler planets of 2.18 and for TESS planets of 1.82.

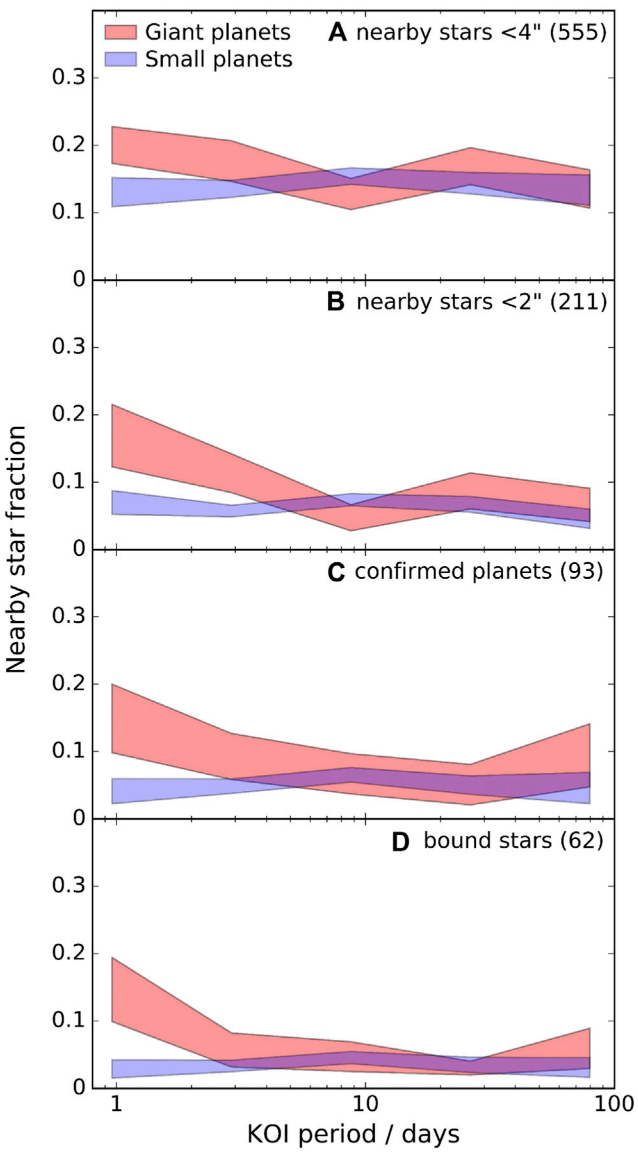

FIGURE 4 | The binary fraction for two planetary populations (giant and small) is shown as a function of orbital period, with 1σ uncertainty regions shaded. The top panel is the original sample, with each subsequent panel removing systems, as described in the text, to clean the sample. In each panel, the number of systems used is shown in parentheses.

Unassociated background or foreground stars are typically found at larger separations from the primary star. If we limit our sample to just TESS systems with separations less than 1″ (to increase the fraction of gravitationally bound companions), we find, using the assumptions of all primary star hosts, all secondary star hosts, and equal mix of primary and secondary star hosts, correction factors of 1.14, 1.90, and 1.55, respectively. The final figure agrees with the correction factor from the Robo-AO survey of Kepler planets of 1.54, as well as from two independent studies of 1.6 (Ciardi et al., 2015) and 1.64 (Hirsch et al., 2017).

In summary, it is clear that the presence of a previously unknown stellar companion has a significant effect on our understanding of any possible planets within the system (increasing their radii by ~60% on average). The composition of smaller planets, in particular, is highly dependent on their estimated radius, particularly if they fall below or above the radius gap at approximately 1.6–1.9 Earth radii (Rogers, 2015; Fulton et al., 2017; Van Eylen et al., 2018) between rocky planets (super-Earths) and those with large gaseous envelopes (sub-Neptunes).

3.3 Giant Planet Migration

It is expected from theoretical planet formation models that the gravitational influence of a stellar companion may drive planets that form at large separations inward, into short-period orbits (Fabrycky and Tremaine, 2007; Katz et al., 2011; Naoz et al., 2012). Smaller planets may be ejected by migrating larger planets in this scenario, resulting in a high fraction of short period giant planets in systems with stellar companions (Xie et al., 2014).

We searched for evidence of these effects using a cleaned sample of binary targets from the Robo-AO Kepler survey, removing known or suspected false positives (Morton and Johnson, 2011; Fressin et al., 2013) and only using likely bound systems as determined by photometric distance estimates Ziegler et al. (2018a).

We find that, after successive cuts to improve the sample (see **Figure 4**), short-period (1–3 days) giant and small planets have a binarity rate of $12.8\%^{+5.6\%}_{-2.8\%}$ and $2.4\%^{+1.8\%}_{-0.9\%}$, respectively. This is a 2.6σ discrepancy between giant and small planets.[1] A significant difference in the binarity rate of the two populations is not found at any other orbital period range.

Ngo et al., (2015) found a similar result in an NIR survey of hot Jupiter hosts, which were twice as likely to have stellar companions as compared to field stars at a 2.8σ significance. The binary fraction found in their survey was significantly higher (51%), likely a result of differences in observational methods and sensitivity (e.g., increased sensitivity in the infrared to M-dwarf companions). The binary fraction for hot Jupiter hosts in the Robo-AO survey is in agreement with the 12% rate found by Roell et al., (2012), who used seeing-limited observations to detect close companions.

3.4 Close Binary Suppression of Planets

A close stellar companion can significantly reduce the probability that planets can form and survive around a star. Yet, we still find planets in close binary systems. We use the data from the SOAR TESS survey to understand how binary stars interact with planetary systems.

Kraus et al., (2016) found that few Kepler host stars are in solar system scale binary systems (separations within 50 AU), implying that planets are significantly less likely to form in these systems. The TESS planets take generally larger and shorter periods than the Kepler planets, due to the reduced photometric precision of TESS and survey strategy. Unlike Kepler, however, the TESS planets are spread across the sky, not in a limited region, and

[1]Errors for both populations are based on Poissonian statistics (Burgasser et al., 2003).

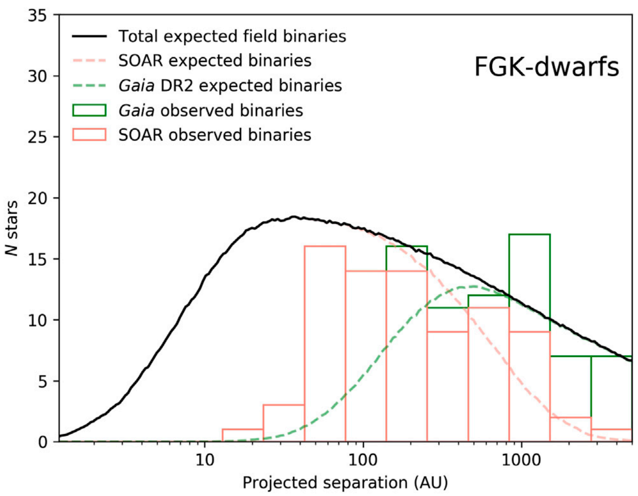

FIGURE 5 | In red and green, the number of observed companions from SOAR and in Gaia DR2 for solar-type TESS planet candidate hosts in logarithmic bins of projected separation of 0.25 dex width. Companions found by both SOAR and Gaia are included in the SOAR sample. In black is the expected distribution from a multiplicity study of field stars (Raghavan et al., 2010), combining both field binaries that would be detected by SOAR and Gaia. The expected binaries from SOAR and Gaia, individually, are also plotted. These distributions take into account the detection sensitivity of both SOAR and Gaia. The observed distribution shows a clear paucity of TESS planet candidate host binaries at projected separations less than ~40 AU compared to the field stars and are consistent with field expectations at wider separations.

allow us to sample a more diverse set of the Galactic stellar population.

Similar to Kraus et al., (2016), we use the field binary statistics of Raghavan et al., (2010) to compare the planet candidate hosting planets. Any differences between the two samples may be a result of planet formation suppression. For this analysis, we first cull the sample of 875 observed TOIs using several parameters (non-Solar type stars, false positives, and high contrast systems) to a final sample consisting of 484 stars. We supplement the SOAR observations with common proper motion pairs found in Gaia DR2 (Gaia Collaboration et al., 2018).

A histogram of the observed distribution of binaries based on projected separation compared to the simulated survey of field stars is shown in **Figure 5**. A deep deficit of observed exoplanet candidate systems with close binaries is apparent, indicating that these systems are treacherous for planet formation and evolution. A simple two-parameter suppression model, a step function reduction in binaries by 90^{+2}_{-3}% at 34^{+9}_{-6} AU physical separation, fits the observed distribution.

The exact mechanism that suppresses the survival of planets in these systems is unclear, but several theories have been put forth. Quintana et al., (2007) suggest that stellar companions may stir planetesimals, increasing their velocity and reducing their density in the protoplanetary disc. Naoz et al., (2012) suggest that binary stars perturb planetary orbits, resulting in tidal migration that can lead to planetary ejection. Jang-Condell et al., (2008) and Kraus et al., (2012) find evidence that stellar companions reduce the material in, and lifetime of, protoplanetary discs. Lastly, Alexander (2012) suggests that the additional radiation from the companion increases photoevaporation in the disc, stripping gaseous planets of their atmospheres. Why can some systems survive while others are destroyed? More observations of these systems (to determine association between the two stars, identify the planet host, and map out physical rather than the snapshot projected separation) and the detection of more systems, particularly close binary systems that do host planets, will likely bring more insight. These systems are relatively rare and serve as the most stringent tests for theoretical formation models.

4 CONCLUSION

The Kepler and TESS missions provided the community the significant challenge of needing thousands of high-resolution images to confirm and characterize exoplanet systems. Robo-AO and SOAR speckle imaging are uniquely suited to perform those observations in a comprehensive and uniform manner. Over four years, Robo-AO imaged nearly all of the Kepler planet candidates. This corrected the planetary radius estimates for over 600 systems and led to the verification of over a thousand planets (Morton et al., 2016). The TESS survey is observing every TESS planet candidate visible from the South. Currently over 800 targets have been observed, with over 200 having nearby companions, and the speckle observations have contributed to the confirmation of over 40 planets [e.g.,Espinoza et al., (2019); Jones et al. (2019); Quinn et al., (2019); Rodriguez et al., (2019); Vanderburg et al., (2019)]. This has resulted in the best evidence yet that close, Solar System scale binary systems suppress planet formation. The TESS survey is ongoing with targets from the extended mission being observed.

Data from the Robo-AO survey of Kepler planet candidate host stars are available at the survey website[2]. Data from the SOAR telescope observations of TESS planet candidate host stars are available on the Exoplanet Follow-up Observation Program website[3].

DATA AVAILABLITY STATEMENT

Publicly available datasets were analyzed in this study. This data can be found here: Kepler ExoFOP.

AUTHOR CONTRIBUTIONS

CZ performed the data reduction for the Robo-AO survey. NL, CB, and RR built and maintained the Robo-AO instrument and ran the observations of the exoplanet hosts. AT performed the speckle observations on the SOAR telescope.

[2]http://roboaokepler.com/.

[3]https://exofop.ipac.caltech.edu/tess/index.php.

FUNDING

This research was supported by the NASA Exoplanets Research Program, grant No. NNX 15AC91G. CZ and WH acknowledge support from the North Carolina Space Grant consortium. TM was supported by NASA, grant No. NNX 14AE11G under the Kepler Participating Scientist Program.

ACKNOWLEDGMENTS

We thank the observatory staff at Kitt Peak for their efforts to assist Robo-AO KP operations and are grateful to the Palomar Observatory staff for their support of Robo-AO on the 1.5 m telescope. The Robo-AO instrument was developed with support from the National Science Foundation under grants AST-0906060, AST-0960343, and AST-1207891, IUCAA, the Mt. Cuba Astronomical Foundation, and by a gift from Samuel Oschin. The Robo-AO team thanks NSF and NOAO for making the Kitt Peak 2.1 m telescope available. Robo-AO KP is a partnership between the California Institute of Technology, the University of Hawai'i, the University of North Carolina at Chapel Hill, the Inter-University Centre for Astronomy and Astrophysics (IUCAA) at Pune, India, and the National Central University, Taiwan. The Murty family feels very happy to have added a small value to this important project. Robo-AO KP is also supported by grants from the John Templeton Foundation and the Mt. Cuba Astronomical Foundation. Some data are based on observations at Kitt Peak National Observatory, National Optical Astronomy Observatory (NOAO Prop. ID: 15B-3001), which is operated by the Association of Universities for Research in Astronomy (AURA) under cooperative agreement with the National Science Foundation. This research used observations obtained at the Southern Astrophysical Research (SOAR) telescope, which is a joint project of the Ministério da Ciência, Tecnologia, Inovações e Comunicações (MCTIC) do Brasil, the U.S. National Optical Astronomy Observatory (NOAO), the University of North Carolina at Chapel Hill (UNC), and Michigan State University (MSU). This article includes data collected by the TESS mission. Funding for the TESS mission is provided by the NASA Explorer Program. This work has made use of data from the European Space Agency (ESA) mission Gaia (https://www.cosmos.esa.int/gaia), processed by the Gaia Data Processing and Analysis Consortium (DPAC, https://www.cosmos.esa.int/web/gaia/dpac/consortium). This research has made use of the Exoplanet Follow-up Observation Program website, which is operated by the California Institute of Technology, under contract with the National Aeronautics and Space Administration under the Exoplanet Exploration Program. This research has made use of the NASA Exoplanet Archive, which is operated by the California Institute of Technology, under contract with the National Aeronautics and Space Administration under the Exoplanet Exploration Program. Facilities: PO:1.5 m (Robo-AO), KPNO:2.1 m (Robo-AO), SOAR (HRCam).

REFERENCES

Adams, E. R., Ciardi, D. R., Dupree, A. K., Gautier, T. N., III, Kulesa, C., and McCarthy, D. (2012). Adaptive optics images of kepler objects of interest. *AJ* 144, 42. doi:10.1088/0004-6256/144/2/42

Adams, E. R., Dupree, A. K., Kulesa, C., and McCarthy, D. (2013). Adaptive optics images. II. 12 kepler objects of interest and 15 confirmed transiting planets. *AJ* 146, 9. doi:10.1088/0004-6256/146/1/9

Alexander, R. (2012). The dispersal of protoplanetary disks around binary stars. *ApJ* 757, L29. doi:10.1088/2041-8205/757/2/L29

Baranec, C., Riddle, R., and Law, N. M. (2017). Automated adaptive optics. ArXiv e-prints. Available at: https://arxiv.org/abs/1709.07103

Baranec, C., Riddle, R., Law, N. M., Chun, M. R., Lu, J. R., Connelley, M. S., et al. (2014a). "Second generation Robo-AO instruments and systems," In *Adaptive optics systems IV* (Bellingham, WA: SPIE), Vol. 9148, 914812. doi:10.1117/12.2055552

Baranec, C., Riddle, R., Law, N. M., Ramaprakash, A. N., Tendulkar, S., Hogstrom, K., et al. (2014b). High-efficiency autonomous laser adaptive optics. *ApJ* 790, L8. doi:10.1088/2041-8205/790/1/L8

Baranec, C., Ziegler, C., Law, N. M., Morton, T., Riddle, R., Atkinson, D., et al. (2016). Robo-AO kepler planetary candidate survey. II. Adaptive optics imaging of 969 kepler exoplanet candidate host stars. *AJ* 152, 18. doi:10.3847/0004-6256/152/1/18

Batalha, N. M., Rowe, J. F., Bryson, S. T., Barclay, T., Burke, C. J., Caldwell, D. A., et al. (2013). Planetary candidates observed by kepler. III. Analysis of the first 16 months of data. *ApJs* 204, 24. doi:10.1088/0067-0049/204/2/24

Borucki, W. J., Koch, D., Basri, G., Batalha, N., Brown, T., Caldwell, D., et al. (2010). Kepler planet-detection mission: introduction and first results. *Science* 327, 977. doi:10.1126/science.1185402

Borucki, W. J., Koch, D. G., Basri, G., Batalha, N., Boss, A., Brown, T. M., et al. (2011a). Characteristics of kepler planetary candidates based on the first data set. *ApJ* 728, 117. doi:10.1088/0004-637X/728/2/117

Borucki, W. J., Koch, D. G., Basri, G., Batalha, N., Brown, T. M., Bryson, S. T., et al. (2011b). Characteristics of planetary candidates observed by kepler. II. Analysis of the first four months of data. *ApJ* 736, 19. doi:10.1088/0004-637X/736/1/19

Gaia CollaborationBrown, A. G. A., Vallenari, A., Prusti, T., de Bruijne, J. H. J., Babusiaux, C., et al. (2018). Gaia data release 2. Summary of the contents and survey properties. *Astron. Astrophys.* 616, A1. doi:10.1051/0004-6361/201833051

Brown, T. M., Latham, D. W., Everett, M. E., and Esquerdo, G. A. (2011). Kepler input catalog: photometric calibration and stellar classification. *AJ* 142, 112. doi:10.1088/0004-6256/142/4/112

Burgasser, A. J., Kirkpatrick, J. D., Reid, I. N., Brown, M. E., Miskey, C. L., and Gizis, J. E. (2003). Binarity in Brown dwarfs: T dwarf binaries discovered with the hubble space telescope wide field planetary camera 2. *ApJ* 586, 512–526. doi:10.1086/346263

Burke, C. J., Bryson, S. T., Mullally, F., Rowe, J. F., Christiansen, J. L., Thompson, S. E., et al. (2014). Planetary candidates observed by kepler IV: planet sample from Q1-Q8 (22 Months). *ApJs* 210, 19. doi:10.1088/0067-0049/210/2/19

Ciardi, D. R., Beichman, C. A., Horch, E. P., and Howell, S. B. (2015). Understanding the effects of stellar multiplicity on the derived planet radii from transit surveys: implications for kepler, K2, and TESS. *ApJ* 805, 16. doi:10.1088/0004-637X/805/1/16

Coughlin, J. L., Mullally, F., Thompson, S. E., Rowe, J. F., Burke, C. J., Latham, D. W., et al. (2016). Planetary candidates observed by kepler. VII. The first fully uniform catalog based on the entire 48-month data set (Q1-Q17 DR24). *ApJs* 224, 12. doi:10.3847/0067-0049/224/1/12

Dressing, C. D., Adams, E. R., Dupree, A. K., Kulesa, C., and McCarthy, D. (2014). Adaptive optics images. III. 87 kepler objects of interest. *AJ* 148, 78. doi:10.1088/0004-6256/148/5/78

Espinoza, N., Brahm, R., Henning, T., Jordán, A., Dorn, C., Rojas, F., et al. (2019). HD 213885b: a transiting 1-day-period super-Earth with an Earth-like composition around a bright (V = 7.9) star unveiled by TESS. *Mon. Not. R. Astron. Soc.* 491 (2), 2982–2999. doi:10.1093/mnras/stz3150

Fabrycky, D., and Tremaine, S. (2007). Shrinking binary and planetary orbits by kozai cycles with tidal friction. *ApJ* 669, 1298–1315. doi:10.1086/521702

Fressin, F., Torres, G., Charbonneau, D., Bryson, S. T., Christiansen, J., Dressing, C. D., et al. (2013). The false positive rate of kepler and the occurrence of planets. *ApJ* 766, 81. doi:10.1088/0004-637X/766/2/81

Fulton, B. J., Petigura, E. A., Howard, A. W., Isaacson, H., Marcy, G. W., Cargile, P. A., et al. (2017). The California-kepler survey. III. a gap in the radius distribution of small planets. *AJ* 154, 109. doi:10.3847/1538-3881/aa80eb

Gaidos, E., Mann, A. W., Kraus, A. L., and Ireland, M. (2016). They are small worlds after all: revised properties of kepler M dwarf stars and their planets. *Mon. Not. Roy. Astron. Soc.* 457, 2877–2899. doi:10.1093/mnras/stw097

Hirsch, L. A., Ciardi, D. R., Howard, A. W., Everett, M. E., Furlan, E., Saylors, M., et al. (2017). Assessing the effect of stellar companions from high-resolution imaging of kepler objects of interest. *AJ* 153, 117. doi:10.3847/1538-3881/153/3/117

Horch, E. P., Howell, S. B., Everett, M. E., and Ciardi, D. R. (2014). Most sub-arcsecond companions of kepler exoplanet candidate host stars are gravitationally bound. *ApJ* 795, 60. doi:10.1088/0004-637X/795/1/60

Horch, E. P., Howell, S. B., Everett, M. E., and Ciardi, D. R. (2012). Observations of binary stars with the differential speckle survey instrument. IV. Observations of kepler, CoRoT, and hipparcos stars from the gemini north telescope. *AJ* 144, 165. doi:10.1088/0004-6256/144/6/165

Howell, S. B., Everett, M. E., Sherry, W., Horch, E., and Ciardi, D. R. (2011). Speckle camera observations for the NASA kepler mission follow-up Program. *AJ* 142, 19. doi:10.1088/0004-6256/142/1/19

Jang-Condell, H., Mugrauer, M., and Schmidt, T. (2008). Disk truncation and planet formation in γ cephei. *ApJ* 683, L191. doi:10.1086/591791

Jensen-Clem, R., Duev, D. A., Riddle, R., Salama, M., Baranec, C., Law, N. M., et al. (2018). The performance of the robo-AO laser guide star adaptive optics system at the Kitt peak 2.1 m telescope. *AJ* 155, 32. doi:10.3847/1538-3881/aa9be6

Jones, M. I., Brahm, R., Espinoza, N., Wang, S., Shporer, A., Henning, T., et al. (2019). HD 2685 b: a hot Jupiter orbiting an early F-type star detected by TESS. *Astron. Astrophys.* 625, A16. doi:10.1051/0004-6361/201834640

Katz, B., Dong, S., and Malhotra, R. (2011). Long-term cycling of kozai-lidov cycles: extreme eccentricities and inclinations excited by a distant eccentric perturber. *Phys. Rev. Lett.* 107, 181101. doi:10.1103/PhysRevLett.107.181101

Kraus, A. L., Ireland, M. J., Hillenbrand, L. A., and Martinache, F. (2012). The role of multiplicity in disk evolution and planet formation. *ApJ* 745, 19. doi:10.1088/0004-637X/745/1/19

Kraus, A. L., Ireland, M. J., Huber, D., Mann, A. W., and Dupuy, T. J. (2016). The impact of stellar multiplicity on planetary systems. I. The ruinous influence of close binary companions. *AJ* 152, 8. doi:10.3847/0004-6256/152/1/8

Law, N. M., Morton, T., Baranec, C., Riddle, R., Ravichandran, G., Ziegler, C., et al. (2014). Robotic laser adaptive optics imaging of 715 kepler exoplanet candidates using robo-AO. *ApJ* 791, 35. doi:10.1088/0004-637X/791/1/35

Lillo-Box, J., Barrado, D., and Bouy, H. (2014). High-resolution imaging of Kepler planet host candidates. a comprehensive comparison of different techniques. *Astron. Astrophys.* 566, A103. doi:10.1051/0004-6361/201423497

Lillo-Box, J., Barrado, D., and Bouy, H. (2012). Multiplicity in transiting planet-host stars. a lucky imaging study of kepler candidates. *Astron. Astrophys.* 546, A10. doi:10.1051/0004-6361/201219631

Marcy, G. W., Isaacson, H., Howard, A. W., Rowe, J. F., Jenkins, J. M., Bryson, S. T., et al. (2014). Masses, radii, and orbits of small kepler planets: the transition from gaseous to rocky planets. *ApJs* 210, 20. doi:10.1088/0067-0049/210/2/20

Mathur, S., Huber, D., Batalha, N. M., Ciardi, D. R., Bastien, F. A., Bieryla, A., et al. (2017). Revised stellar properties of kepler targets for the Q1-17 (DR25) transit detection run. *ApJs* 229, 30. doi:10.3847/1538-4365/229/2/30

Morton, T. D., Bryson, S. T., Coughlin, J. L., Rowe, J. F., Ravichandran, G., Petigura, E. A., et al. (2016). False positive probabilities for all kepler objects of interest: 1284 newly validated planets and 428 likely false positives. *ApJ* 822, 86. doi:10.3847/0004-637X/822/2/86

Morton, T. D., and Johnson, J. A. (2011). On the low false positive probabilities of kepler planet candidates. *ApJ* 738, 170. doi:10.1088/0004-637X/738/2/170

Naoz, S., Farr, W. M., and Rasio, F. A. (2012). On the formation of hot jupiters in stellar binaries. *ApJ* 754, L36. doi:10.1088/2041-8205/754/2/L36

Ngo, H., Knutson, H. A., Hinkley, S., Crepp, J. R., Bechter, E. B., Batygin, K., et al. (2015). Friends of hot jupiters. II. no correspondence between hot-jupiter spin-orbit misalignment and the incidence of directly imaged stellar companions. *ApJ* 800, 138. doi:10.1088/0004-637X/800/2/138

Quinn, S. N., Becker, J. C., Rodriguez, J. E., Hadden, S., Huang, C. X., Morton, T. D., et al. (2019). Near-resonance in a system of sub-Neptunes from TESS. *AJ* 158 (5), 177. doi:10.3847/1538-3881/ab3f2b

Quintana, E. V., Adams, F. C., Lissauer, J. J., and Chambers, J. E. (2007). Terrestrial planet formation around individual stars within binary star systems. *ApJ* 660, 807–822. doi:10.1086/512542

Raghavan, D., McAlister, H. A., Henry, T. J., Latham, D. W., Marcy, G. W., Mason, B. D., et al. (2010). A survey of stellar families: multiplicity of solar-type stars. *ApJs* 190, 1–42. doi:10.1088/0067-0049/190/1/1

Ricker, G. R., Winn, J. N., Vanderspek, R., Latham, D. W., Bakos, G. Á., Bean, J. L., et al. (2014). "Transiting exoplanet survey satellite (TESS)," In Space telescopes and instrumentation 2014: optical, infrared, and millimeter wave, Bellingham, WA, August 28, 2014 (Bellingham, WA: Society of Photo-Optical Instrumentation Engineers (SPIE)), Vol. 9143, 914320. doi:10.1117/12.2063489

Rodriguez, J. E., Quinn, S. N., Huang, C. X., Vanderburg, A., Penev, K., Brahm, R., et al. (2019). An eccentric massive jupiter orbiting a subgiant on a 9.5-day period discovered in the transiting exoplanet survey satellite full frame images. *AJ* 157, 191. doi:10.3847/1538-3881/ab11d9

Roell, T., Neuhäuser, R., Seifahrt, A., and Mugrauer, M. (2012). Extrasolar planets in stellar multiple systems. *A&A* 542, A92. doi:10.1051/0004-6361/201118051

Rogers, L. A. (2015). Most 1.6 earth-radius planets are not rocky. *ApJ* 801, 41. doi:10.1088/0004-637X/801/1/41

Rowe, J. F., Bryson, S. T., Marcy, G. W., Lissauer, J. J., Jontof-Hutter, D., Mullally, F., et al. (2014). Validation of kepler's multiple planet candidates. III. light curve analysis and announcement of hundreds of new multi-planet systems. *ApJ* 784, 45. doi:10.1088/0004-637X/784/1/45

Stassun, K. G., Oelkers, R. J., Paegert, M., Torres, G., Pepper, J., De Lee, N., et al. (2019). The revised TESS input catalog and candidate target list. *AJ* 158 (4), 138. doi:10.3847/1538-3881/aade86

Tokovinin, A. (2018). Ten years of speckle interferometry at SOAR. *PASP* 130, 035002. doi:10.1088/1538-3873/aaa7d9

Van Eylen, V., Agentoft, C., Lundkvist, M. S., Kjeldsen, H., Owen, J. E., Fulton, B. J., et al. (2018). An asteroseismic view of the radius valley: stripped cores, not born rocky. *MNRAS* 479, 4786–4795. doi:10.1093/mnras/sty1783

Vanderburg, A., Huang, C. X., Rodriguez, J. E., Becker, J. C., Ricker, G. R., Vanderspek, R. K., et al. (2019). TESS spots a compact system of super-earths around the naked-eye star HR 858. *Astrophys. J. Lett.* 881 (1), L19. doi:10.3847/2041-8213/ab322d

Wizinowich, P. L., Le Mignant, D., Bouchez, A. H., Campbell, R. D., Chin, J. C. Y., Contos, A. R., et al. (2006). The W. M. Keck observatory laser guide star adaptive optics system: overview. *Publ. Astron. Soc. Pac.* 118, 297–309. doi:10.1086/499290

Xie, J.-W., Wu, Y., and Lithwick, Y. (2014). Frequency of close companions among kepler planets—a transit time variation study. *ApJ* 789, 165. doi:10.1088/0004-637X/789/2/165

Ziegler, C., Law, N. M., Baranec, C., Howard, W., Morton, T., Riddle, R., et al. (2018a). Robo-AO kepler survey. V. the effect of physically associated stellar companions on planetary systems. *AJ* 156, 83. doi:10.3847/1538-3881/aace59

Ziegler, C., Law, N. M., Baranec, C., Morton, T., Riddle, R., De Lee, N., et al. (2018b). Measuring the recoverability of close binaries in Gaia DR2 with the robo-AO kepler survey. *AJ* 156, 259. doi:10.3847/1538-3881/aad80a

Ziegler, C., Law, N. M., Baranec, C., Riddle, R., Duev, D. A., Howard, W., et al. (2018c). Robo-AO kepler survey. IV. the effect of nearby stars on 3857 planetary candidate systems. *AJ* 155 (4), 161. doi:10.3847/1538-3881/aab042

Ziegler, C., Law, N. M., Morton, T., Baranec, C., Riddle, R., Atkinson, D., et al. (2017). Robo-AO kepler planetary candidate survey. III. adaptive optics imaging of 1629 kepler exoplanet candidate host stars. *AJ* 153, 66. doi:10.3847/1538-3881/153/2/66

Ziegler, C., Tokovinin, A., Briceño, C., Mang, J., Law, N., and Mann, A. W. (2020). SOAR TESS survey. I. sculpting of TESS planetary systems by stellar companions. *AJ* 159, 19. doi:10.3847/1538-3881/ab55e9

Conflict of Interest: The authors declare that the research was conducted in the absence of any commercial or financial relationships that could be construed as a potential conflict of interest.